Computer Science and Artificial Intelligence Laboratory

Technical Report

MIT-CSAIL-TR-2006-014 March 1, 2006

A soft touch: Compliant Tactile Sensors for Sensitive Manipulation

Eduardo Torres-Jara, Iuliu Vasilescu, and Raul Coral

massachusetts institute of technology, cambridge, ma 02139 usa — www.csail.mit.edu

A soft touch: Compliant Tactile Sensors for Sensitive Manipulation

Eduardo Torres-Jara, Iuliu Vasilescu
Computer Science and Artificial Intelligence
Massachusetts Institute of Technology
32 Vassar St. 32-380, Cambridge, MA 02139, USA
etorresj@csail.mit.edu, iuliuv@mit.edu

Raul Coral
Sloan Automotive Laboratory
Massachusetts Institute of Technology
77 Mass. Ave. 31-061, Cambridge, MA 02139, USA
raul@mit.edu

***Abstract*— We present the design, analysis and construction of a biologically inspired tactile sensor. The sensor can measure normal and lateral forces, conform to the surfaces with which it comes in contact and increase the friction of the surface for a good grasp.**

The sensor is built using a simple process and the applied forces are read using standard electronics. These features make the sensors ideal for mass production.

We are motivated to build tactile sensors that are useful for robotic manipulation given that the current ones do not have the features that we consider necessary. The sensors presented in this paper have been designed to deal with these issues. They have been designed and implemented in the fingers of the humanoid robot Obrero [12].

***Index Terms*— Compliance. Deformable Tactile Sensor. Biologically inspired.**

I. Introduction

We are motivated to build tactile sensors that are useful for robotic manipulation in unmodeled environments [12]. These sensors should be capable of detecting when a robotic part (i.e. finger, hand, arm, etc) comes in contact with any type of object at any incident angle. This feature is very important because in general a robot will not have any prior model of the object and thus have to use its limbs to come into contact and learn about the object. Moreover, the sensor should have a shape that makes it prone to contact.

Current tactile sensors are not good at detecting generalized contact. For example, consider a computer touch pad that uses force resistor sensors (FSR). These pads have high spatial resolution, low minimum detectable the force (about 0.1N) and a good force range (7 bits). These features make the sensor work very well when a human finger, a plastic pen or another object with a pointy shape comes in contact. However if you place a larger object or the same pen at a small incident angle, it is very unlikely that these contacts are detected unless the applied force is very large.

The detection is even more difficult when this pad is mounted in a low mechanical impedance robotic finger (such as the one in Obrero [12]). This is because the low mechanical impedance makes the finger deflect when it comes in contact with an objet. A tactile sensor on this finger should be able to detect this contact with only a little deflection of the finger, because if the deflection is large, undesired forces are already being applied to the object. Therefore, the sensor needs to be very sensitive and able to detect forces applied from different directions.

Another factor that we consider important for the functionality of the sensor is its shape. The shape should be such that it is physically reachable from a range of directions. In other words, the shape should make the sensor prone to contact. We can observe that in the human skin, where there are hairs and ridges that stick out. That is opposed to the design of a traditional tactile sensor whose shape is planar and only normal forces to its surface will be detectable.

Moreover, after the initial contact with an object, the fingers of a robot exert high forces to handle objects. Consequently, the tactile sensors also need to deal with this condition by either handling saturation or having a large operating range. Lastly, a tactile sensor should be able to conform to the object to increase the friction and facilitate manipulation.

In this paper, we present a biologically inspired tactile sensor which has been designed to deal with the issues described above. Using human skin as inspiration, we designed and built sensors that are prone to contact, can detect contact from different directions and can deform to increase friction. These sensors have been implemented in the fingers of the humanoid robot Obrero. In section II we present a survey of the related work. The design and evaluation are presented in sections III and IV. Finally, section V includes the conclusions.

II. Related Work

Many attempts have been made to implement tactile sensing in robots. There are many technologies used to build sensor arrays: conductive elastomers [11], elastomer-dielectric capacitive [13], optical sensors (surface motion and frustrated internal reflection) [9], piezoelectric [7], acoustic, magnetoelastic, electromagnetic dipoles, silicon micromechanical (mems), and force sensing resistors. A complete review of these technologies can be found in [5]. The performance of these sensors has been measured according to the parameters mentioned in a survey study by Harmon [4]. Those parameters include: spatial and temporal resolution, measurement accuracy, noise rejection, hysteresis, linearity, number of wires, packing, and cost. However, it is not clear if many of these designs are useful

for manipulation because little attention has been given to the data produced by these sensors [5].

Most sensors are essentially a flexible elastic skin, coupled with a method of measuring the deformations caused by the applied force. In [3], an IR emitter and receiver are placed inside cavities of an elastic skin. As the skin deforms, the cavity shape changes resulting in change of the received signal. However, the results on pressure sensitivity are not shown, and the sensor is not able to distinguish the direction from which the pressure is applied. In [9] the idea is taken one step further, a full matrix of such sensors is developed and analyzed, light being routed in and out of the cavities using a matrix of optical fibers, taking out some of the bulk of the sensors. Again, only scalar data is obtained.

An interesting idea for a tactile sensor is described by both Lang [10] and Hristuy [2]. Here the finger is a white flexible membrane with a pattern of black dots or lines drawn on the inside. A light source and a CCD camera are placed inside the finger facing the patterns. Pressure on the membrane result in deformations, which are detected by analyzing the CCD images. Significant processing power is required, and overall the sensor is quite big and expensive.

Another approach for sensing tactile forces has been to use joint torque and force information to recover the normal forces [1] instead of using superficial sensors. Nevertheless, this approach is only able to detect resulting forces as opposed to distributions. Tactile sensors also have been developed using organic materials to print circuits [11]. This approach creates flexible transistors that can be used to develop a flexible skin with high density of touch sensors that can easily be wrapped around manipulator's fingers. The sensor used is a rubber sheet that changes conductivity with deformation, the transistors role is to locally amplify the signal and connect it to the matrix of wires that routes the signals to the controller. While the idea has great potential to be developed, so far the results are modest in terms of sensitivity, they only detect force applied in on direction and the organic technology still needs to be perfected (they are sensitive to oxidation).

A promising tactile sensor is described by Chu [13]. Essentially the skin is padded with rubber cones each placed on top of four capacitive force sensors. Having four sensors under each cone makes the detection of both the perpendicular as well as the sideways force the possible. The results were very encouraging with sub gram forces detected. However the process requires a custom silicon wafer to be made (for the capacitive sensors) and therefore might be prohibitively expensive.

A unidirectional capacitive sensors is described by Voyles [8]. Here an electrorheological gel is placed between the inner and outer membrane padded with electrical contacts. The inner membrane is a hard material (like plastic) while the outer material is elastic (rubber). Again, pressure changes the relative position of the contacts which causes a change of the capacitance. One interesting property of this fluids is the change in viscosity with the electric field applied, opening doors for an adaptive skin strength to the task. Unfortunately no quantitative data on the sensor are published.

III. Analysis and Design

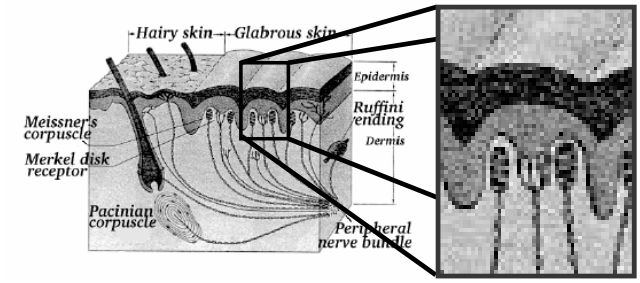

Fig. 1. Detail of the skin. In the magnified view we can observe a curved shape and the lateral sensors that detect its deformation.

In designing the sensor we considered the lessons learned in the robot Obrero. Obrero's hand previously used commercial FSR's pads of high spatial resolution (1000 dot per square inch), however, these sensors presented the problems described in section I: flat shape, rigidness and low friction. Moreover, the tactile sensors did not provide any information when they came in contact with a given object in general. Even though the minimum force to produce a reading is $0.098N$ (as stated in [6]), this only works when applied in a particular direction and with a particular probe (i.e. a finger).

In order to address these problems, we analyzed the human skin as a source of inspiration. In figure 1 a sectional cut of a the skin is presented. We can observe, in the amplified view, that the skin shape is curved. This curve deforms when it comes in contact with an object; the innervations on the sides of the shape detect that deformation which is correlated with the force applied. The deformation also increases the surface of contact between the skin and the object, therefore increasing the friction.

Based on this mechanism, we build dome-like shapes using silicon rubber and measure magnitudes related to the deformation to determine the forces applied. We started by analyzing the behavior of the dome in simulation.

A. Simulation analysis

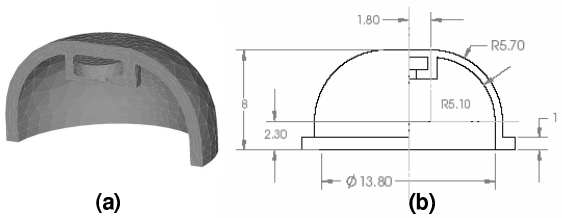

Fig. 2. (a) Meshed geometry for the FEA. (b) Dimensions in mm of the rubber dome.

In order to determine the relation between the load applied to the dome and its deformation, a model to do finite element analysis (FEA) was implemented in ADINA 8

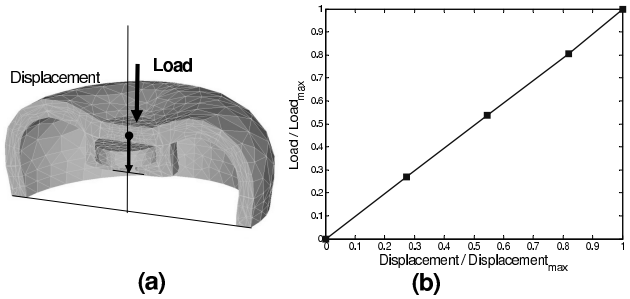

Fig. 3. (a) Deformed mesh under normal force acting on top of the dome. (b) Load versus displacement when force acts on top of the dome. The displacement of top of the dome is measured from its initial position (no load) to its final position (equilibrium with the load applied). The load is applied to the center of the magnet holder. The displacement is normalized by the maximum dome displacement of $5mm$ and the load is normalized by the maximum load of $0.147N$.

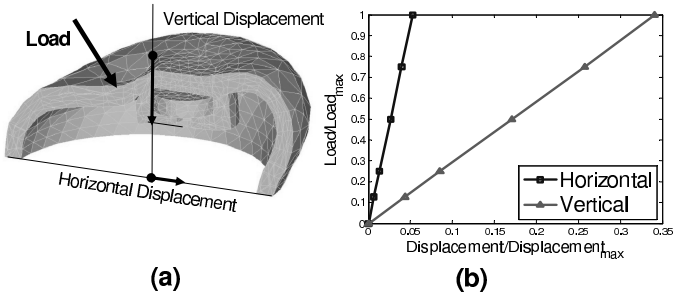

Fig. 4. (a) Deformed geometry under a load acting normal to the surface 45 degrees away from the top of the dome. (b) Load versus displacements. The horizontal displacement is measured from the center of the dome. The vertical displacement is measured at the top of the dome as in the previous case. The displacements are normalized by the maximum horizontal displacement of $7.5mm$ and the maximum vertical displacement of $5mm$. The load value on the plot corresponds to the total force applied. The load is normalized by the maximum vertical load of $0.147N$

(See figure 2a). The specifications of the dome are shown in figure 2b. The dome has a flat surface on top and a circular profile on the sides. Under the flat surface there is a magnet that it will be used for detecting the deformation. The magnet was modelled as a rigid object.

Two types of forces acting on the dome were evaluated: a normal force acting on the top of the dome and a normal force to the surface acting at 45 degrees away from the top of the dome. The base of the dome was fixed. The sensor material was assumed to be isotropic. The stress and strain constitutive relation was assumed to be linear due to the small loads applied to the dome. The values for the material properties were modulus of Young $1.5 \times 10^6 Pa$, Poisson ratio 0.45, and density of $1100 kg/m^3$. For the first load case, normal force applied on the top and the dome downwards displacement as a function of the applied load was determined. The maximum dome displacement is constrained by the base of the sensor which is at $5mm$ from the top of the dome. It was determined that the maximum displacement is achieved under a load of $0.147N$. The resulting dome displacement due to a load is showed in figure 3.

Similarly, for the case where the force acts 45 degrees away from the top of the dome, the relations of the horizontal displacement vs. load and the vertical displacement vs. load were determined. The horizontal displacement is measured from the center of the dome. The vertical displacement is measured from the top of the dome (when no load is applied) downwards. The displacements are normalized by the maximum horizontal displacement of $7.5mm$ and the maximum vertical displacement of $5mm$. The load is normalized by the maximum vertical load of $0.147N$. Figure 4 illustrates the deformed geometry and the load/displacement relations.

The FEA shows that there is a linear relation between the displacement and load and that the dome can detect forces acting at various locations of its surface. Parameters that have not been explored are the dome thickness and curvature; these parameters should allow tuning of the sensor to detect a force.

B. Design

The dome shape shown in figures 2 and 5 was used as the basic shape for the sensors. This dome deforms when either lateral or normal forces are applied as shown in the section III-A. The force needed to deform the dome is determined by the structure and the material used to build the sensor. According to the FEA, there is a linear relation between the displacement and the load. Given that the FEA does not cover all the possibilities, this linear relation might not hold for all the forces applied. However, we can assume that measuring the displacement of the center of the dome will give us a reasonable estimation of the forces applied.

In the design process, we considered a number of methods for determining the displacement of the center of the dome, i.e. using magnetic, optical, and pressure sensors. We chose to use the magnetic approach in our primary design and evaluation. We also implemented the optical method and showed some preliminary evaluation in section IV. Lastly, we implemented and discussed the pressure method. In the following sections, we describe each method.

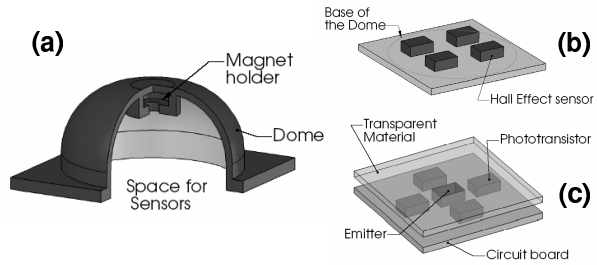

Fig. 5. (a) Cut of the silicon rubber dome. The base of the dome is glued to a circuit board with electronics that measures the deformation. (b) Diagram of the circuit board using hall effect sensors to measure the deformation. This board goes under the dome. (c) Diagram of the circuit board using light to measure the deformation. For this case a dome without the magnet holder was built.

1) Magnetic: In this approach, we embed a magnet in the top of the dome. The base of the dome is glued to a printed circuit board (PCB). The magnetic field of the magnet is detected by 4 hall effect sensors on the PCB (figure 5b). The difference on the signal detected

by the sensors will give a rough approximation of lateral displacement and the average of the signals will give the vertical displacement. When the top of the dome reaches the base of the dome, no more displacement will be allowed and the sensor saturates. Additional sensors can be placed in the PCB to measure beyond this saturation limit. Each one of the hall effect sensors is multiplexed and read through and A/D converter. This converter is part of 16F876A PIC microcontroller that transmits the information via RS232 using ASCII code. Four of these domes were used in each falange of the fingers in the robot Obrero (see figure 11). Obrero's hand has 24 domes in its fingers and 16 in its palm.

It is important to note that the sensitivity of the sensor can be controlled by changing the shape of the domes. More easily deformable structures can be created to satisfy a given application. In figure 6, we present an example of a more sensible sensor that consists of only one dome as opposed to four as in the previous case. There are four magnets embedded in the structure which allows detect the deformation. These structure is easily deformable because a larger surface is supported by farther away walls. However, independently of the shape, the problem with this sensing method is that it is affected by metallic objects. Therefore we also experimented using light and pressure for detecting the deformation.

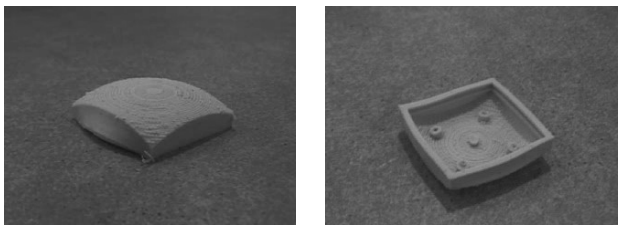

(a) (b)

Fig. 6. (a) The shape of this dome is a spherical surface intersected with a cube. This surface deforms with less force than the previous shape considered. (b) We can observe the magnets on the other side of the dome.

2) Optic: The dome used for optical detection is like the one shown in figure 5 except that the magnet holder was removed. The base of the dome is glued to a printed circuit board (PCB) which has one light emitter and 4 phototransistors as shown in figure 5c. The total power reflected gives the vertical deformation of the dome and the difference between the sensors signals gives the lateral deformation. A transparent layer was added to prevent the dome from completely blocking the light emitter and guarantee a monotonic reading of the light reflection. This layer will also be the limit of the vertical displacement of the dome. The force that produces such deformation is the saturation threshold of the sensor.Therefore, this layer will deal with forces greater than the saturation limit. As in the previous case, the output of each of the phototransistors goes to a multiplexor connected to an A/D converter which is part of a 16F876A PIC microcontroller.

3) Pressure: Another implementation was to seal the domes with air in their interior and place a pressure sensor on their base. The pressure was measured using a ICS1451 sensor. The drawback of this approach is that it does not differentiate horizontal from vertical displacement. Moreover, pressure sensors need more complicated and more expensive electronics than the previous methods. Therefore, we did not completely characterize this type of sensor.

C. Material and molding

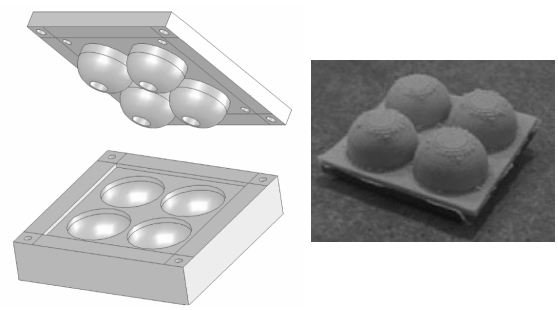

(a) (b)

Fig. 7. (a) CAD rendering of the mold used to build 4 sensors. The dimensions were chosen to fit the fingers of the robot Obrero. (b) Four domes molded using silicon rubber.

The sensors were built using Freeman V-1062 room-temperature, condensation-cured silicone, which is very simple to use without expensive tooling. This material was chosen because of its very low hardness (14 Shore A), good tensile strength (545 PSI) and tear resistance (120 ppi). The molds were constructed using a 3D printer. In figure 7 we can see one of those molds.

IV. Evaluation

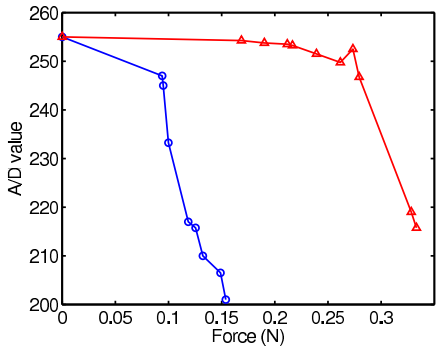

Fig. 8. Response of the magnetic sensor to a vertical force. The figure shows the average of the readings from 4 hall effect sensors as the force applied changes.Each hall effect sensor is read by a 8 bit A/D converter. The dome is composed of spherical part with a flat circular surface on the top (figure 2b). The behavior of the dome is different depending on the relative size of the object in contact with respect to the circular surface. The lines with circular and triangular marks show, respectively, the responses to probes smaller and larger than the circular surface of the dome.

As mentioned above, we implemented and evaluated two approaches for determining the displacement of the center

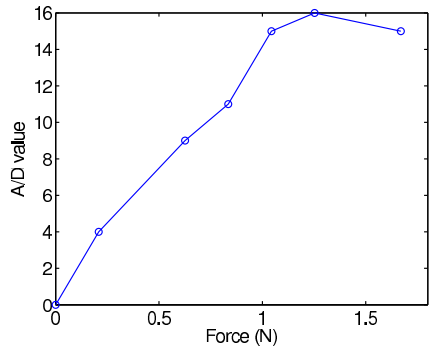

Fig. 9. Response of the magnetic sensor to lateral forces. As shown in figure 5b, the hall effects are organized in a 2 by 2 array. The data presented in this figure is the difference of the two columns. The value of each column is the summation of the readings in that column. The readings come from a 8 bit A/D converter that digitalizes the multiplexed sensor outputs. The direction of the force applied was normal to the columns of hall effects.

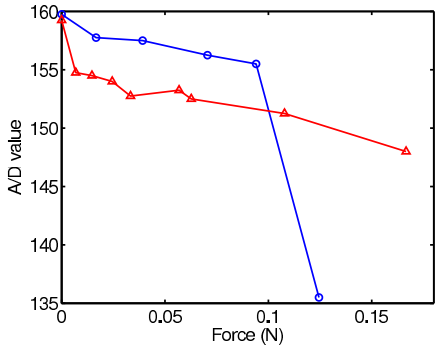

Fig. 10. Response of the optical sensor to a vertical force. The figure shows the average of the readings from 4 photo transistors as the force applied changes. Each phototransistor effect sensor is read by a 8 bit A/D converter. The dome is composed of spherical part with a flat circular surface on the top (figure 2b with no magnetic holder). The behavior of the dome is different depending on the relative size of the object in contact with respect to the circular surface. The lines with circular and triangular marks show, respectively, the responses to probes smaller and larger than the circular surface of the dome.

of the dome, i.e. using magnetic and optical sensors. In this section, we will first present the experimental results of our primary design using the magnetic approach. We then show some preliminary results of the sensors using optical sensors.

1) Magnetic: We apply normal and lateral forces and record the displacement of the center of the dome. The displacement is determined by measuring the intensity of the magnetic field that reaches the hall effect sensors in the base of the dome. The configuration of the hall effect sensors are shown in figure 5b.

We first evaluated the response of the sensor to normal forces. Different weights were applied to the top of the dome using plastic holders. Two cases were considered; holders with contact surfaces smaller and larger than the top surface of the dome. Figure 8 shows the average of the reading of 4 hall effect sensors as the normal forces applied change. The reading of each hall effect sensor is

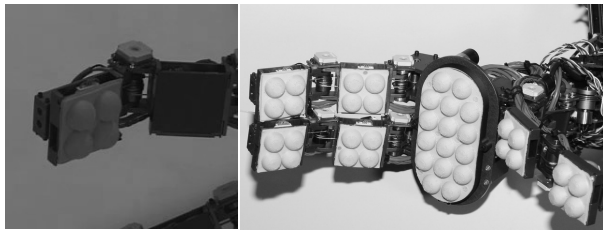

(a) **(b)**

Fig. 11. (a) A four dome tactile sensor mounted in the finger tip of the robot Obrero. (b) Hand of the robot Obrero with 8 domes mounted in each of its 3 finger and 16 on its palm.

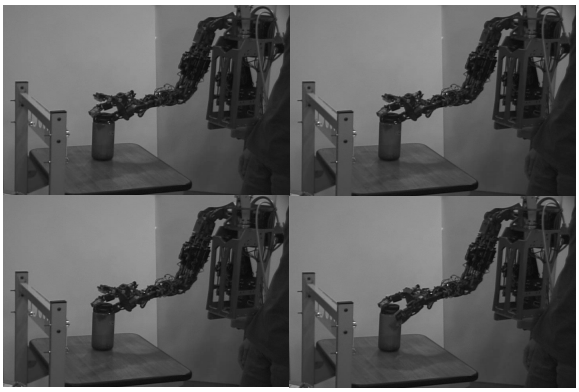

Fig. 12. From left to right and from top to bottom, we present the robot Obrero moving its hand until a contact with a bottle occurs. The task is performed with no help from vision. In the top-left picture, the hand is approaching to the bottle. In the top-right picture, the sensor touches the bottle. In the bottom-left picture, the sensor is being deformed further.In the last picture, the thumb of the robot is moved to the side as a response to the touch. We should notice that the plastic bottle has little mass and it has not been tilted by the contact with the hand.

obtained using a 8 bit A/D converter. The lines with circular and triangular marks show, respectively, the responses to weights whose contact surface are smaller and larger than the circular surface of the dome.

We observe that the readings decrease monotonically in each of the two cases. The relation is not linear as shown in the simulation because the relation between the intensity of the magnetic field and the distance to the hall effects is not linear.

These two different behaviors are determined by the shape of the dome which is composed of a spherical part with a flat circular surface on the top. If the sensor shape were a semi-sphere it would be more difficult to deform and if it were a plane it will be easier. The current one is a combination of both of them. These shape makes the deformation of the sensor greater when it comes in contact with pointy objects. In the simulation analysis, only the case with a contact surface smaller than the top of the dome was considered since we wanted to have a general idea of the behavior of the structure.

In order to determine the response to lateral forces, an array of four domes (see figure 7b) were placed upside down against a flat surface and weight was applied on top of them. These provide a minimum normal force that remained constant. The motion of the array was restricted

to one direction by placing fixed plates on two opposed sides of the array. A lateral force was applied by a cable attached to the side of the array of 4 domes in the unrestricted direction. The cable was routed through a pulley and attached to a weight. The weight applied determines the pulling force.

The lateral displacement is determined by computing the difference among the readings of the hall effect sensors. The sensors whose output is greater have the magnet closer to them. Figure 9 shows the computed difference between the readings of two groups of two sensors for a lateral force of known direction. We can observe that the response curve is roughly monotonic. The minimum normal force detected by the magnetic sensor is $0.094N$. The maximum deflection is obtained when a force of $0.147N$ is applied to the center of the circle in top of the dome and the weight was smaller than the dome.

Certainly many tactile sensors have good sensitivity but they may not necessarily work well on a real robot. These sensors were mounted on the fingers of Obrero's hand (see figure11). In figure 12 we show a sequence of the robot approaching a cylindrical object whose physical characteristics are: $mass = 0.179Kg$, $diameter = 92mm$, $height = 216mm$. When Obrero performs a blind (no vision involved) exploration task and touches the object, it is not pushed or tilted. The tactile sensors deform and conform to the surface of the object. Consequently the hand touches the object gently. Regretly, it is difficult to see all these effects in the figure.

2) Optic: As mentioned above, the second method used to measure the deformation was optic. A LED and 4 photo-transistors were placed in the base of the dome (figure 5c). The same two cases as in the magnetic method were considered. Figure 10 shows the results of this evaluation. The values on the vertical axis are the average of the readings from 4 photo transistors. As in the magnetic case, the lines with circular and triangular marks show, respectively, the responses to weights smaller and larger than the circular surface of the dome. The response to lateral forces was not evaluated for this version.

V. Conclusions

We have presented in this paper the design, analysis, constructions and experimental evaluation of a biologically-inspired tactile sensor. Our sensor has five key properties that make it better suited for manipulation than previous designs. It conforms to the surfaces with which it comes in contact by elastic deformation, enabling the grabbing of a wider range of objects. Its shape make it prone to contact which create the opportunity to sense the environment. It is sensitive to both normal and lateral forces, providing better feedback to the host robot about the object to be grabbed. It has a high sensitivity, enabling its use in state of the art manipulation fingers, which typically have low mechanical impedance - in order to be very compliant. We showed in this paper the integration of our sensor with Obrero's hand [12]. Last but not least the construction of the sensor is simple, using inexpensive technologies like silicon rubber molding and standard stock electronics.

While some of these feature are present in previous designs, none of previous sensors has encompassed all of them. Additionally most of the previous sensor are not fully characterized experimentally, and therefore estimating there usefulness in robotic manipulation is difficult.

Acknowledgment

This work was partially funded by NASA under the NASA ES&RT EPC2132 grant and by ABB . We would like to thank to Tina Wen and Carrick Detweiler and Keith Kotay for their great help on printing the molds and molding the several prototypes. Finally, I would like to thank to Lorenzo Natale for helping testing the sensors on the robot and Alberto Ortega for helping with the simulations.

References

[1] A. Bicchi, J.K. Salisbury, and D.L. Brock. Contact sensing from force measurements. *International Journal of Robotics Research*, 12(3):249–262, June 1993.

[2] Roger W. Brockett Dimitris Hristuy, Nicola Ferrier. The performance of a deformable membrane tactile sensor basic results on geometrically defined tasks. *Int'l Conf. on Robotics and Automation*, 2000.

[3] Andrew Russell Greg Hellard. A robust, sensitive and economical tactile sensor for a robotic manipulator. *Australian Conference on Robotics and Automation*, 2002.

[4] L. D. Harmon. Automated tactile sensing. *International Journal of Robotics Research*, 1(2):3–32, 1982.

[5] Robert D. Howe and Mark R. Cutkosky. *Touch Sensing for Robotic Manipulation and Recognition*, pages 55–112. The Robotics Review 2. O Khatib, J.J. Craig and T. Lozano-Perez. MIT Press, Cambridge, Massachusetts, 1992.

[6] Interlink Electronics, Inc, 546 Flynn Road, Camarillo, CA 93012. *Integration Guide*, 1998. P/N 90-65801 Rev. C.

[7] Helge Ritter Jan Jockusch, Jorg Walter. A tactile sensor system for a three-fingered robot manipulator. *Int. Conf. on Robotics and Automation*, 1997.

[8] Richard M. Voyles Jr., Gary Fedder, and Pradeelp K. Wlosla. Design of a modular tactile sensor and actuator based on an electrorheological gel. *Int'l Conf. on Robotics and Automation*, 1996.

[9] Pencilla Lang. Design and prototyping of a fibre optic tactile array. *The Journal of High School Science*, November 2002.

[10] Pencilla Lang. Optical tactile sensors for medical palpation. *Canada-Wide Science Fair*, May 2004.

[11] Takao Someya, Yusaku Kato, Tsuyoshi Sekitani, Shingo Iba, Yoshiaki Noguchi, Yousuke Murase, Hiroshi Kawaguchi, and Takayasu Sakurai. Conformable, flexible, large-area networks of pressure and thermal sensors with organic transistor active matrixes. *Proc. of National Academy of Sciences*, August 2005.

[12] Eduardo Torres-Jara. Obrero: A platform for sensitive manipulation. In *Proceedings of the IEEE-RAS International Conference on Humanoid Robots*, 2005.

[13] S. Middelhoek Z. Chu, P.M. Sarro. Silicon three-axial tactile sensor. *International Conference on Solid-State Sensors and Actuators*, 1995.